

## Chapter 4

### Experimental Results

#### 4.1 Microstructure of Test Specimens

As-cast microstructures of test specimens are shown in Fig. 4-1-1 for 0.5%C, Fig. 4-1-2 for 1.0%C and Fig. 4-1-3 for 1.5%C specimens, respectively. Also, SEM microphotographs of the same specimens are shown in Fig. 4-2-1 for 0.5%C, Fig. 4-2-2 for 1.0%C and Fig. 4-2-3 for 1.5%C specimens. All the specimens are hypoeutectic. By comparing the optical and SEM microphotographs, the microstructures of 0.5%C-irons consist of primary phases and small of eutectic carbides precipitated at their boundary. The matrix microstructure of specimen No.1 with 1%V is bainitic and/or martensitic and matrix near eutectic transforms into pearlite. In the matrix of specimen No.2 with 2%V, minute carbides are precipitated. Though a specimen with 3%V had been prepared for this experiment, it was not availed because of ferritic matrix in as-cast state. In a family of 1.0%C-irons, the volume fraction of carbides which precipitate on the boundary of primary phases rises. In the primary matrix, bainite and martensite co-exist and they increase in the volume with an increase in V content, and a little more austenite retains in the matrix near the eutectic. In 1.5%C-irons, the eutectic carbides increase and more martensite than bainite appear clearly in the primary matrix, and simultaneously more retained austenite exist in each specimen with different V content.

#### 4.2 Identification of Precipitated Carbides in As-cast Specimen

As for the multi-component white cast iron in which the eutectic carbide is more coarser comparatively, the types of precipitated carbides

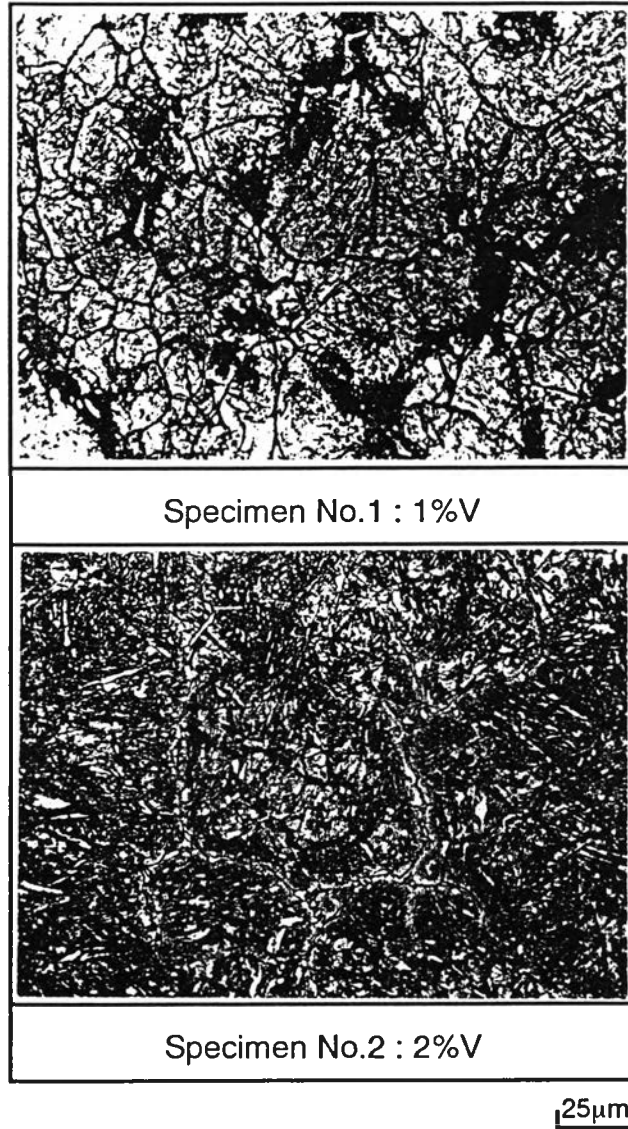


Fig.4-1-1 Optical microphotographs of as-cast specimens with 0.5%C.

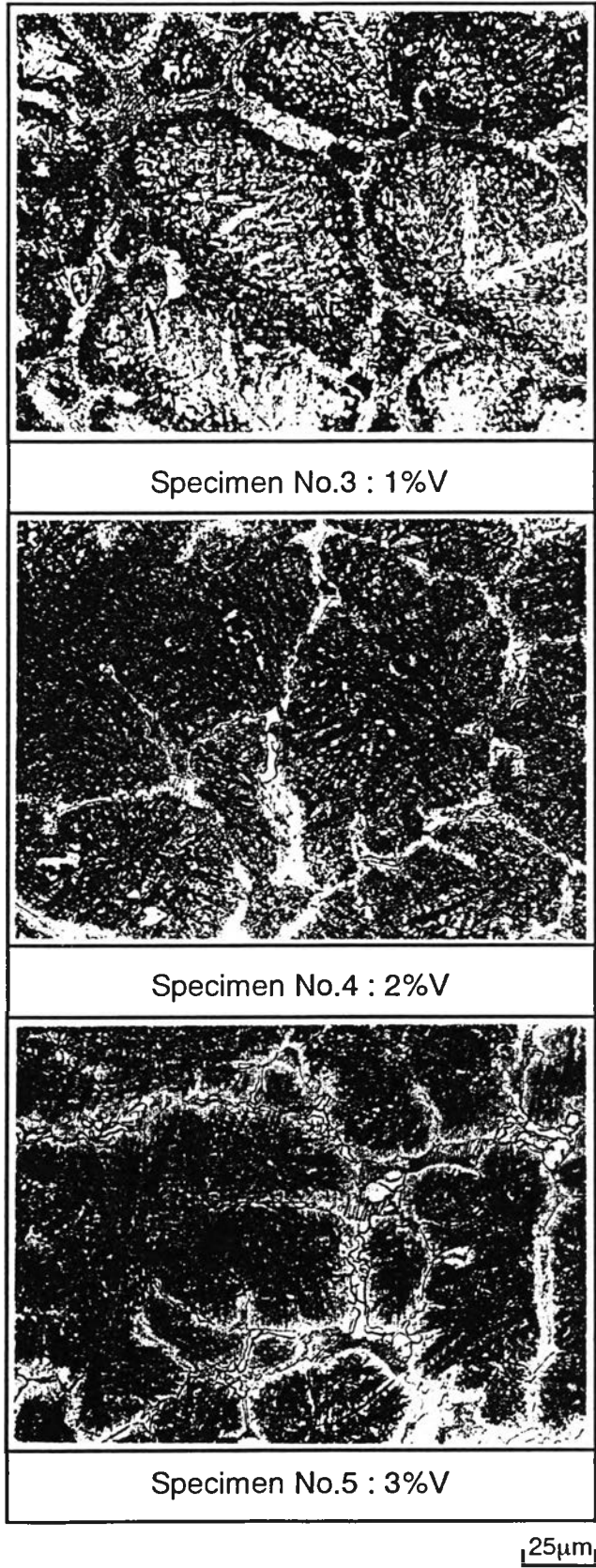
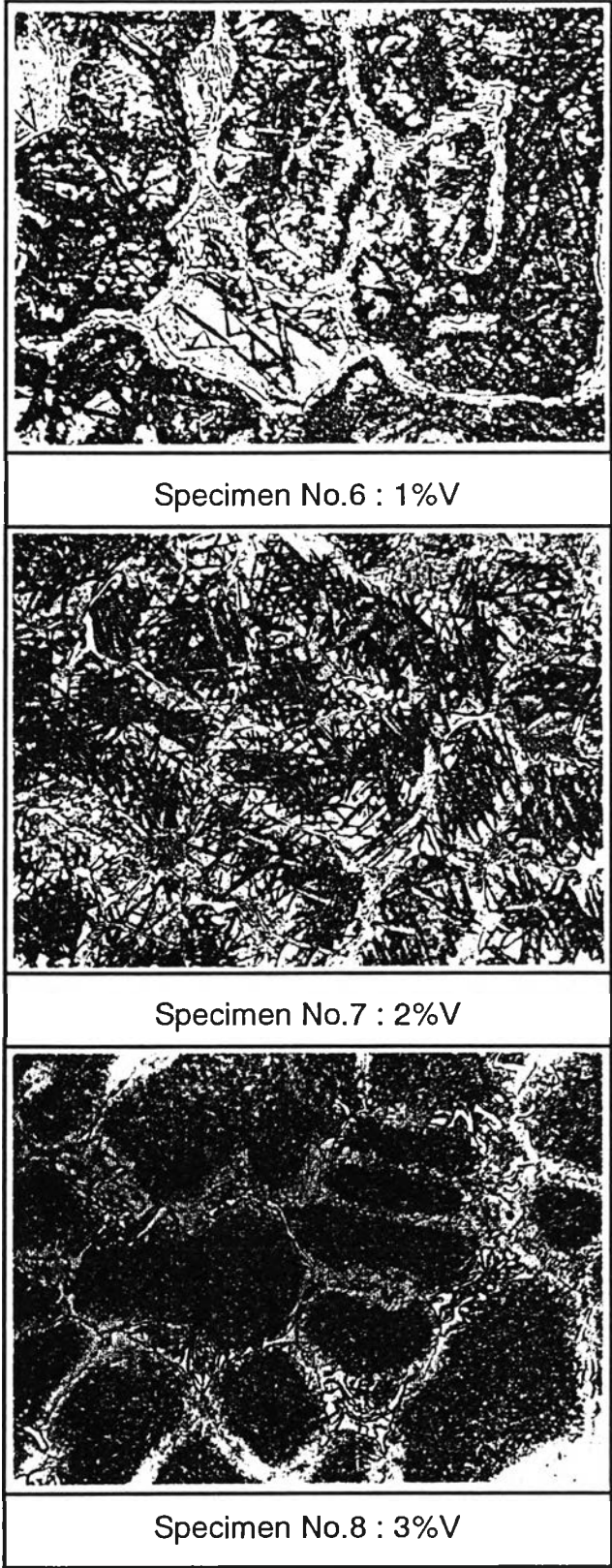


Fig.4-1-2 Optical microphotographs of as-cast specimens with 1.0%C.



25μm

Fig.4-1-3 Optical microphotographs of as-cast specimens with 1.5%C.

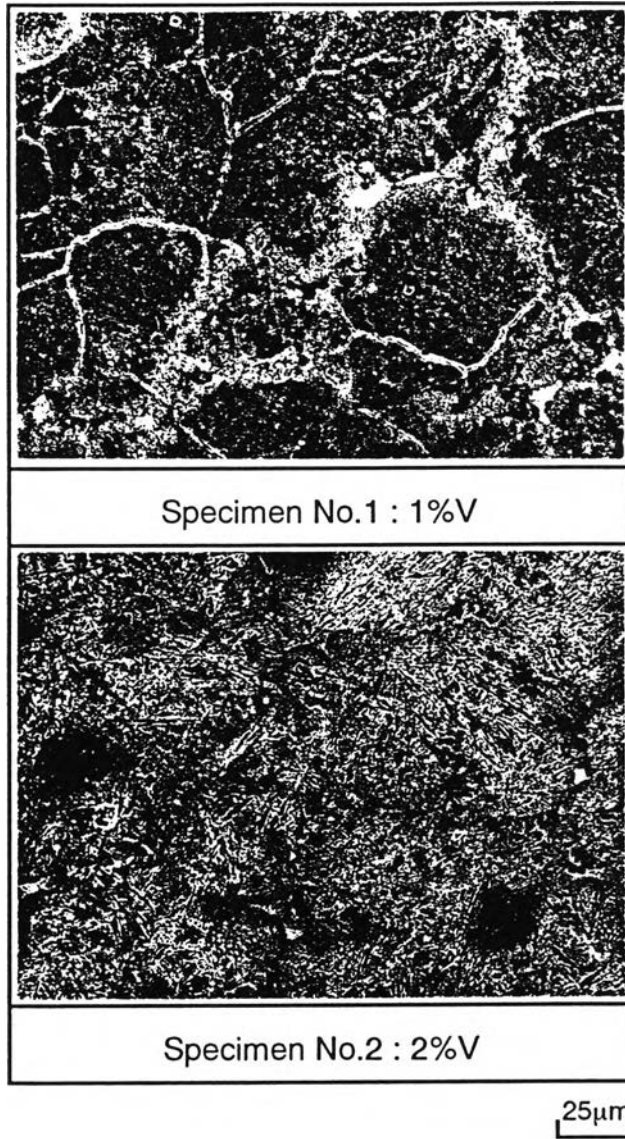


Fig.4-2-1 SEM microphotographs of as-cast specimens with 0.5%C.

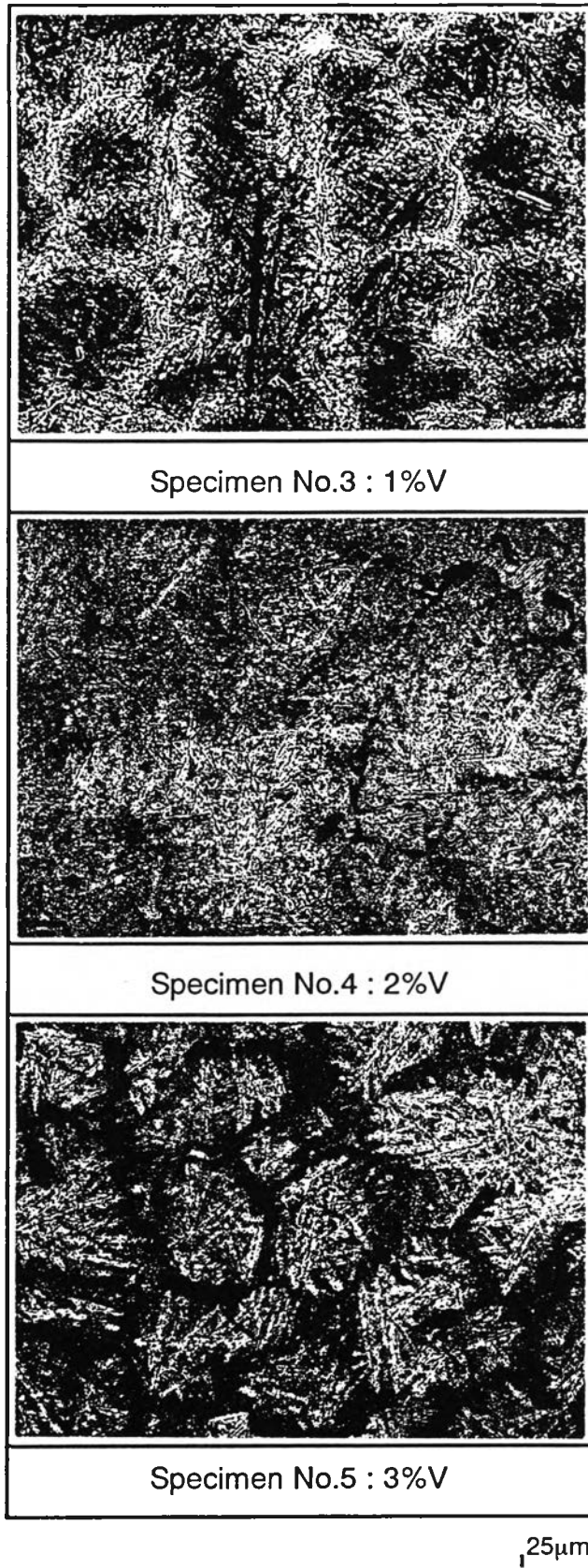


Fig.4-2-2 SEM microphotographs of as-cast specimens with 1.0%C.



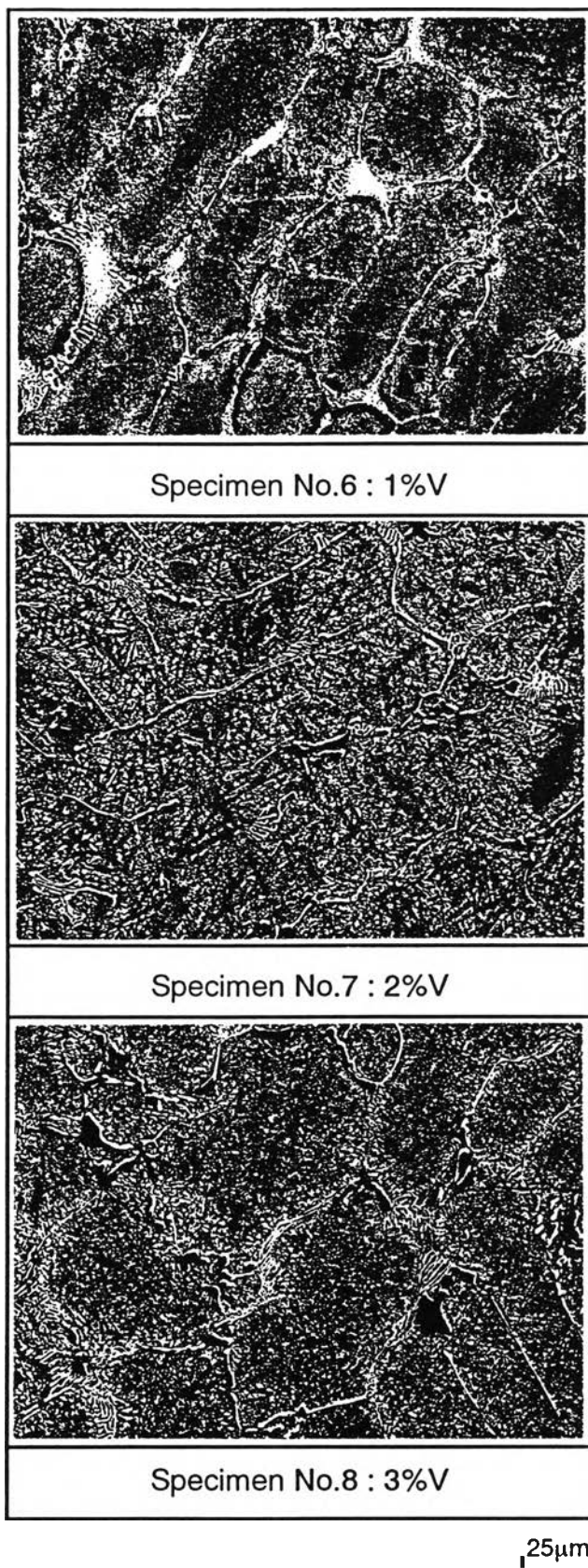


Fig.4-2-3 SEM microphotographs of as-cast specimens with 1.5%C.

have been identified by the methods such as X-ray diffraction<sup>4)</sup>, EPMA quantitative analysis of alloys in carbide<sup>1), 4)</sup> and coloring by etchant<sup>9)</sup>, and now it is roughly possible to estimate the type of carbide from its morphology and chemical composition of the cast iron.

With respect to the specimens used in this research, it was impossible to identify the carbides by X-ray diffraction method because of small amount and minute carbides due to lower C content. Therefore, the coloring method by Murakami etchant was carried out and an example is shown representatively in Fig. 4-3.

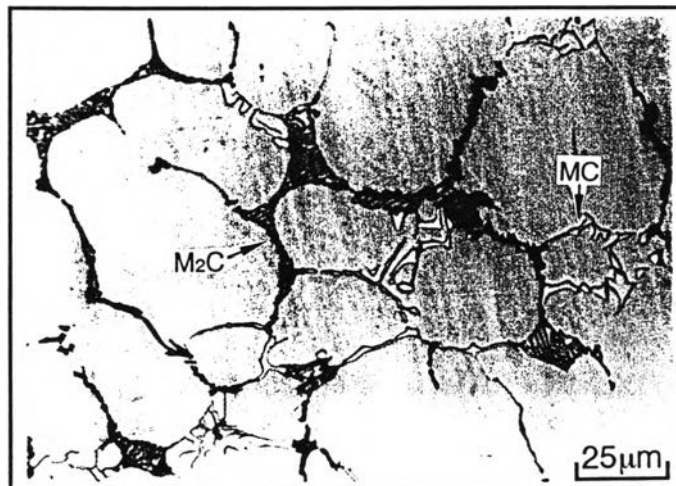


Fig. 4-3 Microphotograph of as-cast specimen No.4 in which MC and  $M_2C$  carbides are distinguished by Murakami etchant.

In all the specimens, massive and flaky carbides with white color (not attacked by the etchant) and black colored carbides in the eutectic existing at the boundary of primary dendrite are observed. As Murakami etchant attacks  $M_2C$ ,  $M_6C$  and  $M_7C_3$  carbides and does not attack MC carbide, it is possible that white carbides are MC type and black ones are  $M_2C$  type. In order to make them sure, the concentration of alloying elements in carbides of 2%V specimens in each C level was quantitatively measured by EDS of EPMA. The results are shown in Table 4-1, white



carbides contain 38-55%V, 22-34%Mo, 6-8%Cr and 5-26%Fe, and alloy concentration of black carbides is 7-13%V, 44-54%Mo, 12-18%Cr and 15-35%Fe. These values are similar to those of MC and M<sub>2</sub>C carbides precipitated in high C multi-component white cast iron<sup>1), 4)</sup>, and then it can be said that white and black carbides are MC and M<sub>2</sub>C types, respectively.

Table 4-1 Alloy concentration in carbides and matrix of multi-component white cast iron

Specimen	Phase	Element (mass%)			
		Cr	V	Mo	Fe
No.2 (0.5%C-2%V)	MC	6.1-6.3	44.9-51.8	25.9-30.1	12.0-20.6
	M <sub>2</sub> C*	-	-	-	-
	Matrix	4.7-5.1	1.8-1.9	4.1-4.4	87.5-88.4
No.4 (1.0%C-2%V)	MC	6.4-6.7	53.7-54.5	22.9-33.5	5.2-16.8
	M <sub>2</sub> C	12.3-17.7	7.7-12.9	44.3-53.4	15.7-35.1
	Matrix	4.2-4.3	1.3-1.5	3.0-3.3	90.0-90.5
No.7 (1.5%C-2%V)	MC	6.7-7.5	38.2-46.6	23.4-30.7	17.3-25.2
	M <sub>2</sub> C	14.1-16.0	9.8-10.7	47.8-53.9	20.0-27.2
	Matrix	4.0-4.1	1.1-1.2	2.3-2.6	91.3-91.7

\*In specimen No.2, M<sub>2</sub>C carbide is too small to be analyzed.

### 4.3 Relationship between Hardness and Volume Fraction of Retained Austenite

#### 4.3.1 As-cast State

Hardness and volume fraction of retained austenite ( $V_\gamma$ ) of the multi-component white cast irons in as-cast state are shown in Table 4-2. The hardness decreases as V content increases in 0.5%C- and 1.0%C-specimens and reversely increases in 1.5%C-specimens. On the other hand,  $V_\gamma$  reduces in each C%-specimens as V content increases and at the same V level,  $V_\gamma$  increases as C content rises.

Table 4-2 Volume fraction of retained austenite ( $V_\gamma$ ) and hardness of as-cast specimens

Specimen	Element (mass%)		HV30	$V_\gamma$ , %
	C	V		
No.1	0.5	1	722	4.7
No.2		2	536	3.1
No.3	1.0	1	782	27.5
No.4		2	724	9.4
No.5		3	614	8.2
No.6	1.5	1	463	84.6
No.7		2	650	51.7
No.8		3	772	28.8

### 4.3.2 As-hardened State

The hardness and  $V_\gamma$  of as-hardened specimens are shown in Table 4-3. In case of 1273 K austenitizing, the hardness of 0.5%C- and 1.0%C-specimens decreases with an increase in V content and that of 1.5%C-specimens show almost same value not related to the V content. In case of 1373 K austenitizing, the hardness decreases in 0.5%C-specimens, almost the same in 1.0%C-specimens and rises in the 1.5%C-specimens as V content increases. The  $V_\gamma$  decreases with an increase in V content regardless of the austenitizing temperature and C content of specimen.

Table 4-3 Volume fraction of retained austenite ( $V_\gamma$ ) and hardness of as-hardened specimens

Specimen	Element (mass%)		Austenitizing Temperature (K)			
	C	V	1273		1373	
			HV30	$V_\gamma$ , %	HV30	$V_\gamma$ , %
No.1	0.5	1	667	1.4	767	5.9
No.2		2	545	1.8	639	1.2
No.3	1.0	1	839	14.3	732	28.6
No.4		2	802	3.5	790	12.4
No.5		3	686	0.9	743	3.3
No.6	1.5	1	801	34.2	502	72.5
No.7		2	850	24.4	635	48.1
No.8		3	832	13.6	741	27.5

### 4.3.3 Tempered State

After the specimens were air-hardened from two austenitizing temperatures of 1273 K and 1373 K, they were tempered at several temperatures from 623 K to 923 K. Relationships between macro-hardness and  $V\gamma$  and tempering temperature are shown in Fig. 4-4 and Fig. 4-5 for 0.5 %C-specimens, in Fig. 4-6 to Fig. 4-8 for 1.0%C-specimens and Fig. 4-9 to Fig. 4-11 for 1.5%C-specimens, respectively. In the diagrams, hardness of as-hardened specimens are plotted for comparison. The curves of the tempered hardness showing the secondary hardening which is usually seen in highly alloyed tool steels, were obtained in each specimen.

In 0.5%C-1%V specimen (No.1) shown by Fig. 4-4, the hardness of specimen quenched from 1273 K and 1373 K are 667HV and 767HV. The hardness lowers once due to the tempering, and increases as the tempering temperature rises. Maximum tempered hardness ( $H_{Tmax}$ ) of 657 HV in 1273 K austenitized and 773 HV in 1373 K austenitized specimens are obtained at the tempering temperatures of 773 K and 798 K, respectively, and the higher austenitizing temperature the higher the  $H_{Tmax}$ . The hardness decreases gradually after showing the  $H_{Tmax}$  regardless of austenitizing temperature, as the tempering temperature increases. The  $V\gamma$  within 2% in 1273 K austenitized specimen disappears all at the tempering temperature of 770 K. When the austenitizing temperature rises up to 1373 K, 6% of  $V\gamma$  exists in as-hardened state, it lowers as the tempering temperature rises and then it becomes nil or 0% at 800 K.

In 0.5%C-2%V specimen (No.2) by Fig. 4-5, hardness in as-hardened state are 545 HV at 1273 K and 639 HV at 1373 K austenitizing. The curves of tempered hardness are overall located at lower hardness side than that of 1%V specimen, and  $H_{Tmax}$  are 582 HV in 1273 K austenitized and 677 HV in 1373 K austenitized specimens. The  $V\gamma$  are less than 2% in both specimens tempered even at the temperatures lower

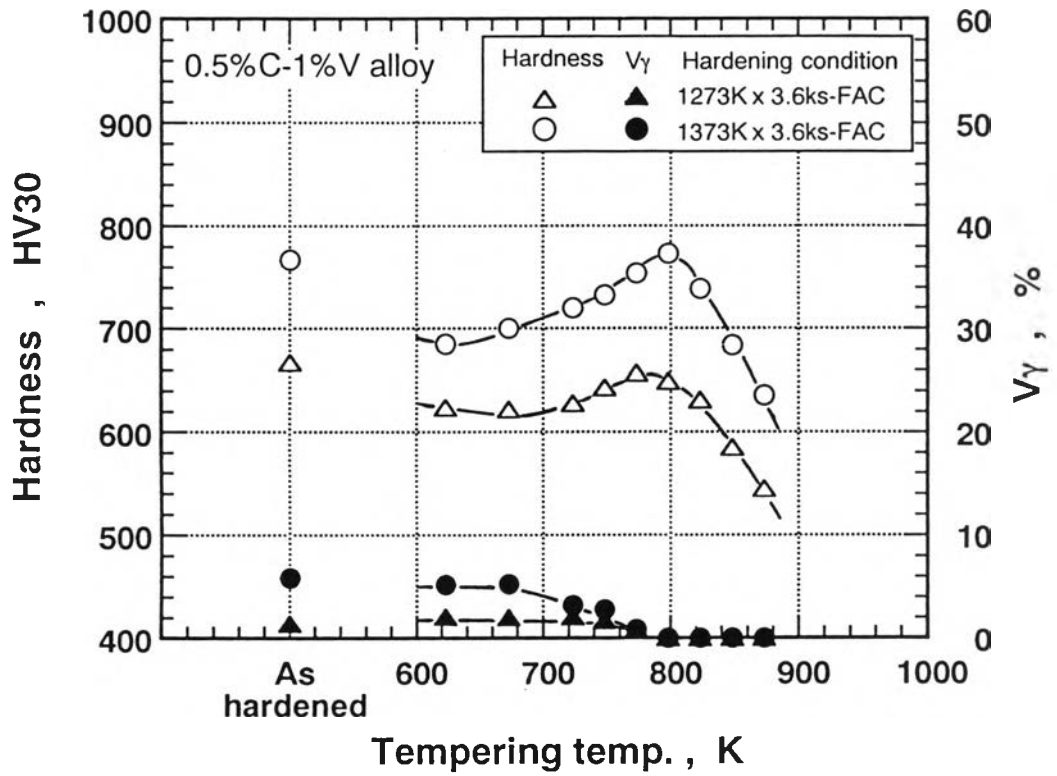


Fig. 4-4 Relationship between macro-hardness and volume fraction of retained austenite( $V_{\gamma}$ ) and tempering temperature. (Specimen No.1)

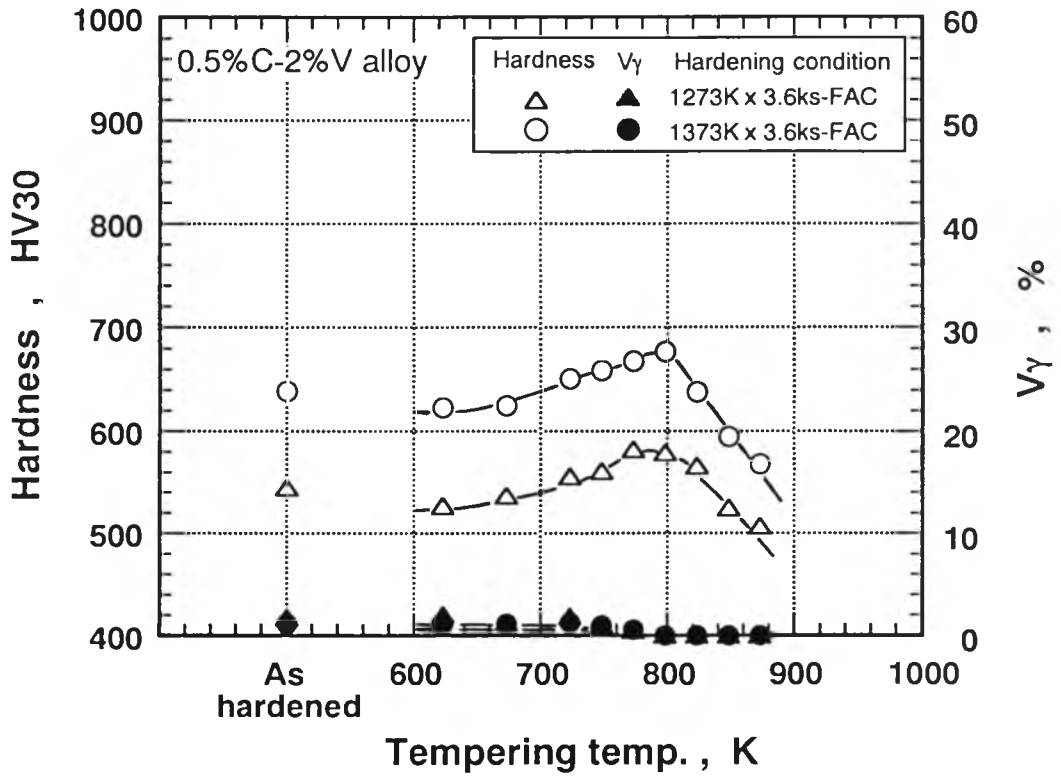


Fig. 4-5 Relationship between macro-hardness and volume fraction of retained austenite( $V_{\gamma}$ ) and tempering temperature. (Specimen No.2)

than 800 K and they disappear perfectly over the 800 K.

The curves of tempered hardness of 1.0%C-1%V specimen (No.3) are shown in Fig. 4-6. As-hardened hardness is 839 HV in 1273 K austenitizing and it also higher than 732 HV in 1373 K austenitizing. The hardness curves show same tendency as those of 0.5%C-specimens. In the temperature range up to 773 K, however, the tempered hardness at higher austenitizing temperature is lower in comparison with those in lower austenitizing temperature of 1273 K, and they are reversed over 773 K. Same tendency can be seen in the tempering curves of 1.5%C-specimens which contained high  $V\gamma$  in as-hardened state and will be described later. The  $H_{T_{max}}$  in 1273 K austenitizing is 778 HV but the one in 1373 K austenitizing is 838 HV. This fact tells that the ratio of secondary precipitation hardening is larger in the specimen austenitized at higher temperature. In as-hardened state, the 14% and 29%  $V\gamma$  exist in 1273 K and 1373 K austenitizing, respectively. They start to decrease gradually over 700 K and the tempering temperatures at 0%  $V\gamma$  are 770 K in 1273 K and 880 K in 1373 K austenitizing, that is, the temperature at which the retained austenite disappears is high in higher austenitizing temperature. This behavior corresponds well with the variation of  $H_{T_{max}}$ .

As for 1.0%C-2%V specimen (No.4) by Fig. 4-7, the hardness in as-hardened state are about same between both of the austenitizing temperatures, 802 HV and 790 HV in 1273 K and 1373 K, respectively. The shapes of tempered hardness curves are similar to the others.  $H_{T_{max}}$  of 829 HV is much higher than that of 743 HV and the  $H_{T_{max}}$  of specimen quenched from higher austenitizing temperature is more.  $V\gamma$  values in as-hardened state are 4% at 1273 K and 12% at 1373 K austenitizing temperatures. Both of the  $V\gamma$  values do not change until 723 K and then gradually reduce with an increase in the tempering temperature. At last, the  $V\gamma$  values become 0% at 770 K in 1273 K and 800 K in 1373 K austenitizing. When the hardness is corresponded to the  $V\gamma$ , it is



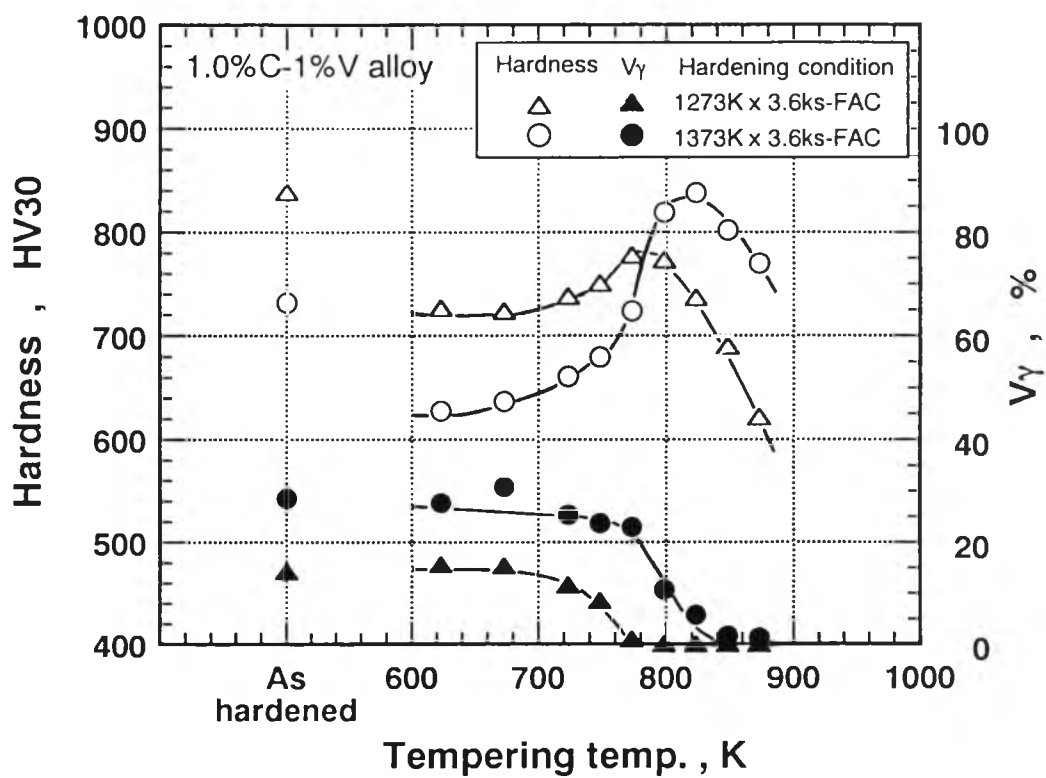


Fig. 4-6 Relationship between macro-hardness and volume fraction of retained austenite( $V_\gamma$ ) and tempering temperature. (Specimen No.3)

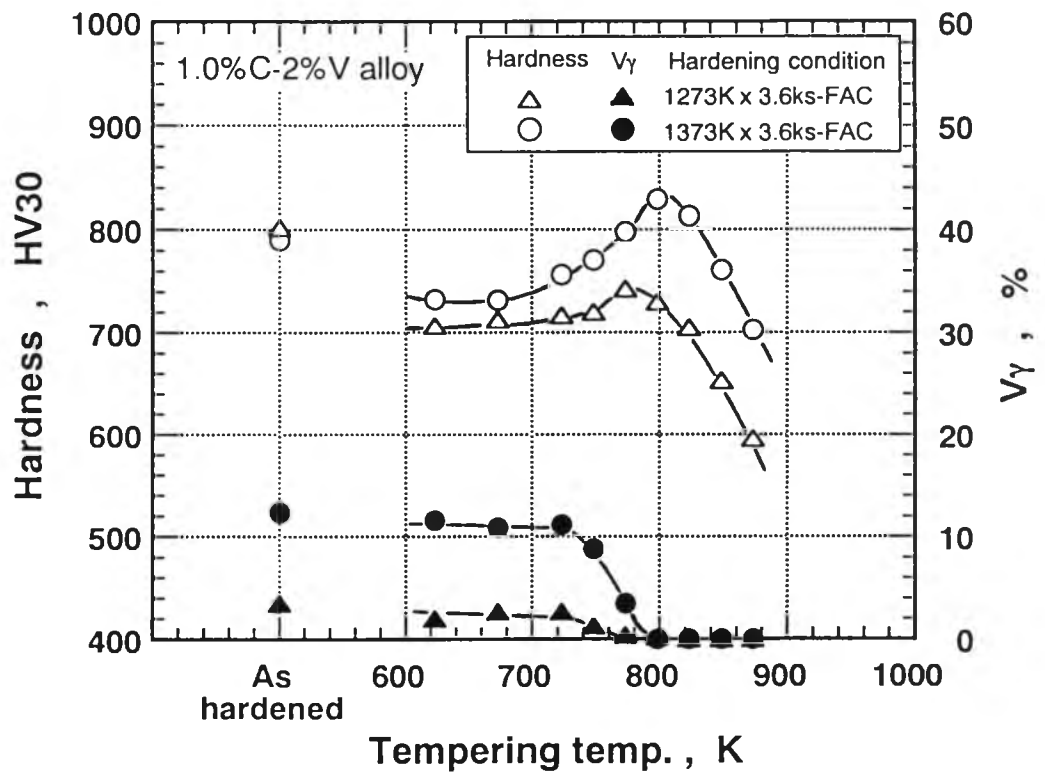


Fig. 4-7 Relationship between macro-hardness and volume fraction of retained austenite( $V_\gamma$ ) and tempering temperature. (Specimen No.4)

understood that the  $H_{T_{max}}$  can be obtained near the tempering temperature at which the retained austenite is gone.

As shown in Fig. 4-8, the hardness of 3%V specimen (No.5) quenched from the high austenitizing temperature of 1373 K is 743 HV which is more than 686 HV of the specimen quenched from low temperature of 1273 K and both of the specimens show secondary precipitation hardening during tempering. However, each  $H_{T_{max}}$  of 694 HV and 760 HV obtained at 773 K in 1273 K austenitizing and 798 K in 1373 K austenitizing show almost the same hardness as the hardness of as-hardened specimen.  $V_{\gamma}$  are already less than 4% in as-hardened specimens, the reason for a little degree of precipitation hardening is considered to be due to less  $V_{\gamma}$  in as-hardened state. In this a series of 1.0%C-specimen quenched from 1273 K, it is clarified that the more V content, the less the hardened hardness and  $V_{\gamma}$ , and resultantly  $H_{T_{max}}$  becomes low. At 1373 K austenitizing, on the other hand,  $H_{T_{max}}$  decreases also despite that  $V_{\gamma}$  of as-hardened specimen decreases as V content increases.

In case of 1.5%C-specimens, it is clear from Fig. 4-9 to Fig. 4-11 that secondary precipitation hardening occurs remarkably regardless of V content. The hardness of specimens quenched from 1273 K and 1373 K are 801 HV and 502 HV in 1%V specimen (No.6), 850 HV and 635 HV in 2%V specimen (No.7) and 832 HV and 741 HV in 3%V specimen (No.8), respectively. On the curves of tempered hardness, 1%V specimen shows  $H_{T_{max}}$  of 826 HV and 723 HV in 1273 K and 1373 K austenitizing temperatures, respectively. On the other hand,  $V_{\gamma}$  of 1%V specimen quenched from 1273 K is 34% and the one quenched from 1373 K is 73%. Such  $V_{\gamma}$  decreases a little until the tempering temperature of 723 K and it begins to decrease gradually by exceeding 723 K. The tempering temperature at which retained austenite disappears is 950 K in 1373 K austenitizing and it is 100 K higher than 850 K in 1273 K austenitizing.

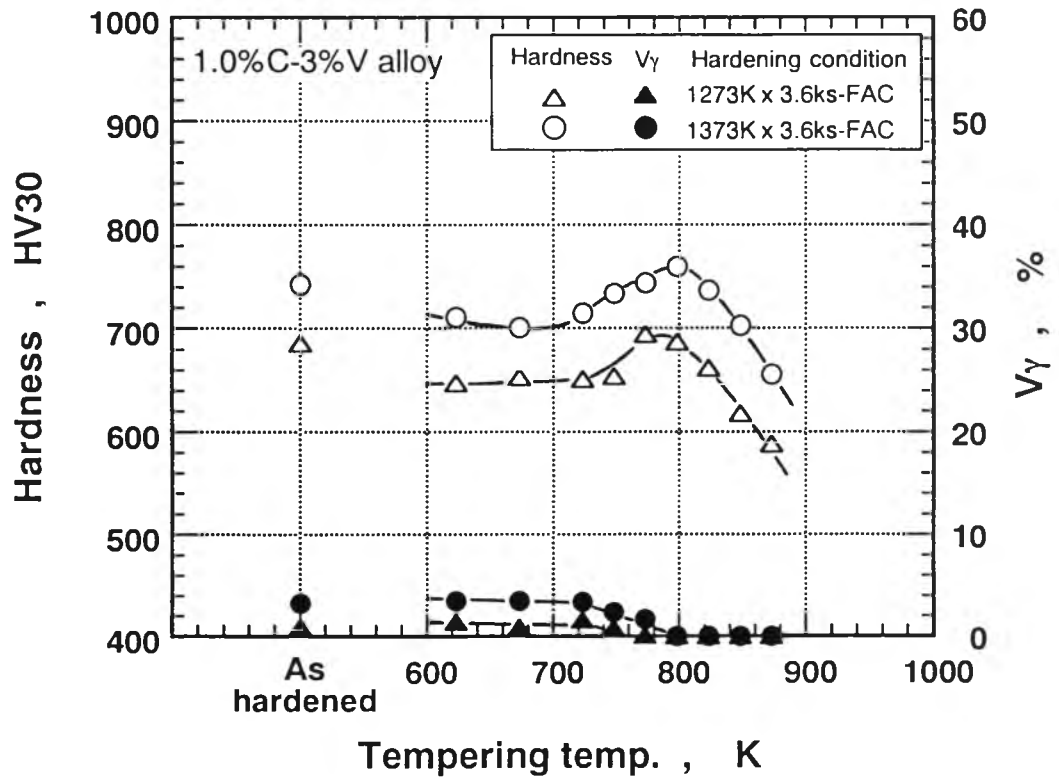


Fig. 4-8 Relationship between macro-hardness and volume fraction of retained austenite( $V_{\gamma}$ ) and tempering temperature. (Specimen No.5)

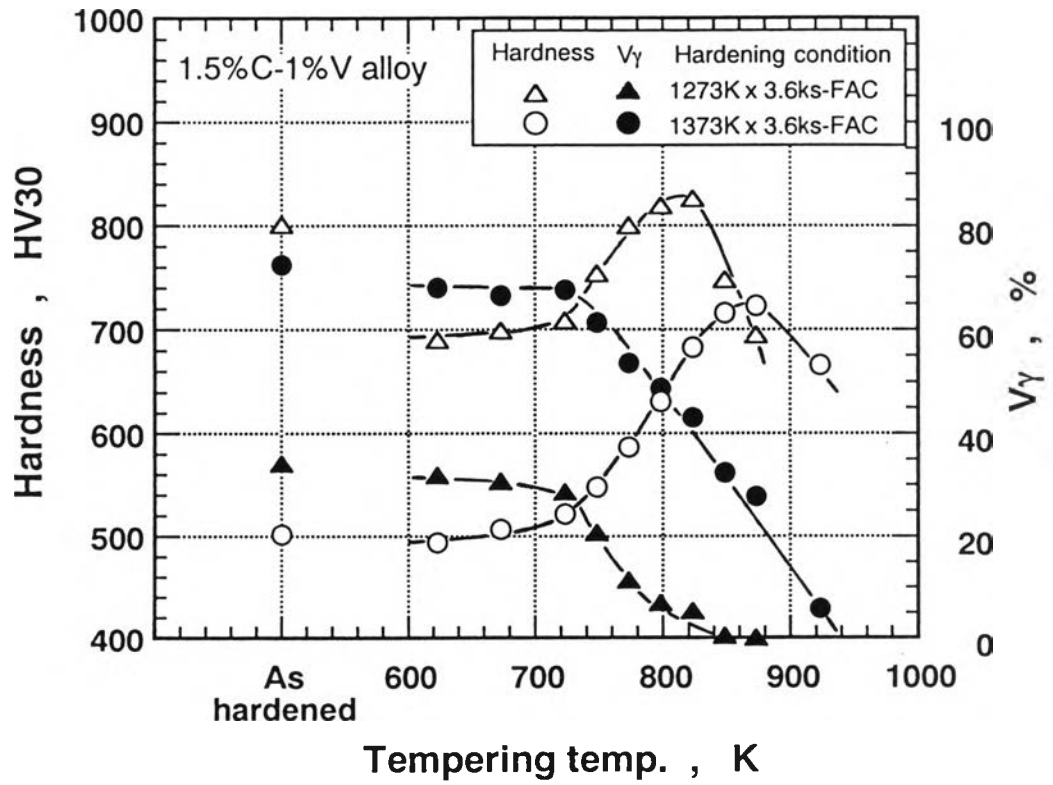


Fig. 4-9 Relationship between macro-hardness and volume fraction of retained austenite( $V_\gamma$ ) and tempering temperature. (Specimen No.6)

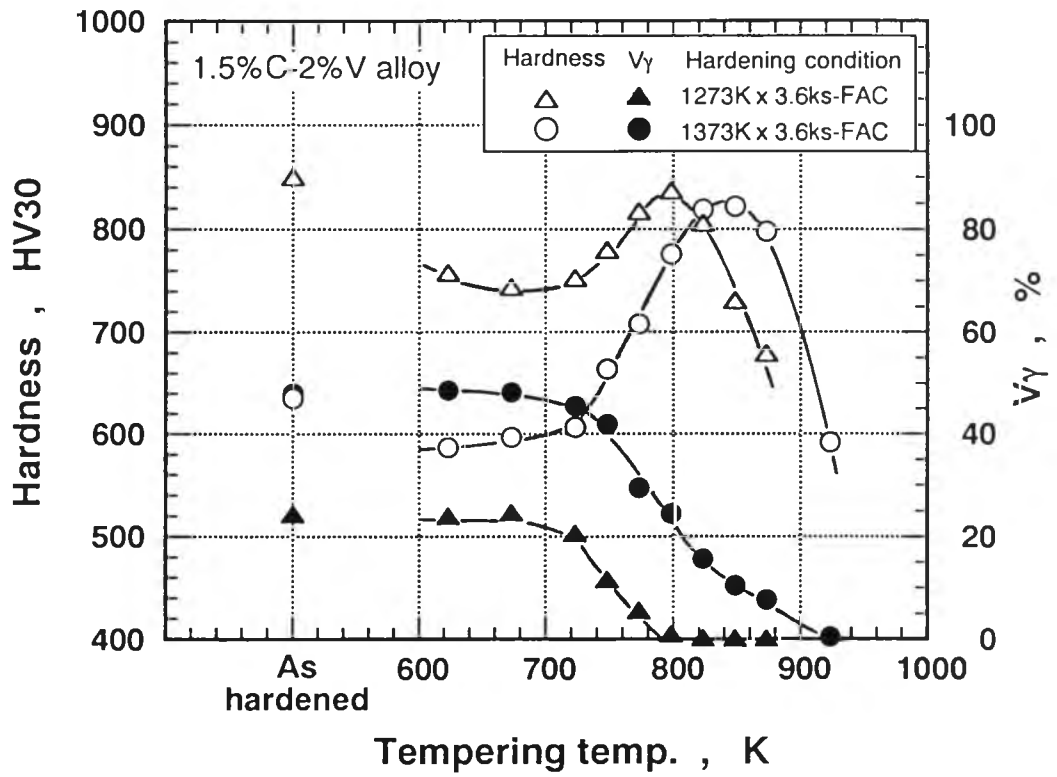


Fig. 4-10 Relationship between macro-hardness and volume fraction of retained austenite( $V_{\gamma}$ ) and tempering temperature. (Specimen No.7)

$H_{T_{max}}$  of 2%V specimen is 837 HV in 1273 K and 822 HV in 1373 K austenitizing temperatures.  $V_{\gamma}$  is 24% in 1273 K and 48% in 1373 K austenitizing. 2%V specimen as well as 1%V specimen shows more retained austenite in the higher austenitizing temperature of 1373 K. The tempering temperature at which  $V_{\gamma}$  gets to 0% is 800 K in 1273 K and 920 K in 1373 K austenitizing and it moves to the high temperature side as the  $V_{\gamma}$  in as-hardened state increases.

As shown in Fig. 4-11, the  $H_{T_{max}}$  of 3%V specimen is 816 HV in 1273 K and 866 HV in 1373 K austenitizing, the tempering temperature at  $H_{T_{max}}$  is shifted to higher temperature side in the specimen with more retained austenite quenched from 1373 K. The curves of tempered hardness of this 3%V specimen behave in a same manner as 1.0%C-1%V specimen.  $V_{\gamma}$  starts to decrease at 748 K and becomes 0% at 800 K in 1273 K and 840 K in 1373 K austenitizing, and the  $V_{\gamma}$  is less than 4% when  $H_{T_{max}}$  is obtained in each specimen. It is noted that 1.5%C-specimens have a certain amount of retained austenite even when they take the  $H_{T_{max}}$  in 1373 K austenitizing and the amount decreases in the order of 28%, 11% and 4% with an increase in V content.

#### **4.4 Relationship between Macro-hardness, Micro-hardness of Matrix and Tempering Temperature**

What is transformed by heat treatment is the matrix. So, the micro-hardness of the matrix was measured using a micro-vickers hardness tester. The comparison of micro-hardness in the matrix with macro-hardness that was described in the clause 4.3.3 is shown in Fig. 4-12 and Fig. 4-13 (0.5%C-specimens), from Fig. 4-14 to Fig. 4-16 (1.0%C-specimens) and Fig. 4-17 to Fig. 4-19 (1.5%C-specimens). In every specimen, the macro-hardness near peak is always higher than the micro-hardness. This suggests that the macro-hardness displays the total



hardness of matrix and eutectic carbides. With respect to the tempered specimens, the difference between macro-hardness and micro-hardness at  $H_{T_{max}}$  is 20-30 HV at 1273 K and 25-60 HV at 1373 K austenitizing temperatures in 0.5%C-specimens, about 50 HV at 1273 K and 45-65 HV at 1373 K austenitizing temperatures in 1.0%C-specimens and 40-65 HV at 1273 K and 20-65 HV at 1373 K austenitizing temperatures in 1.5%C-specimens. Since the change in micro-hardness associated with tempering temperatures shows very similar behavior to that in macro-hardness, it can be allowed that the behavior of the macro-hardness is directly connected to the transformation of matrix. Therefore, the discussions on hardness in the following sections are all carried out using the macro-hardness.

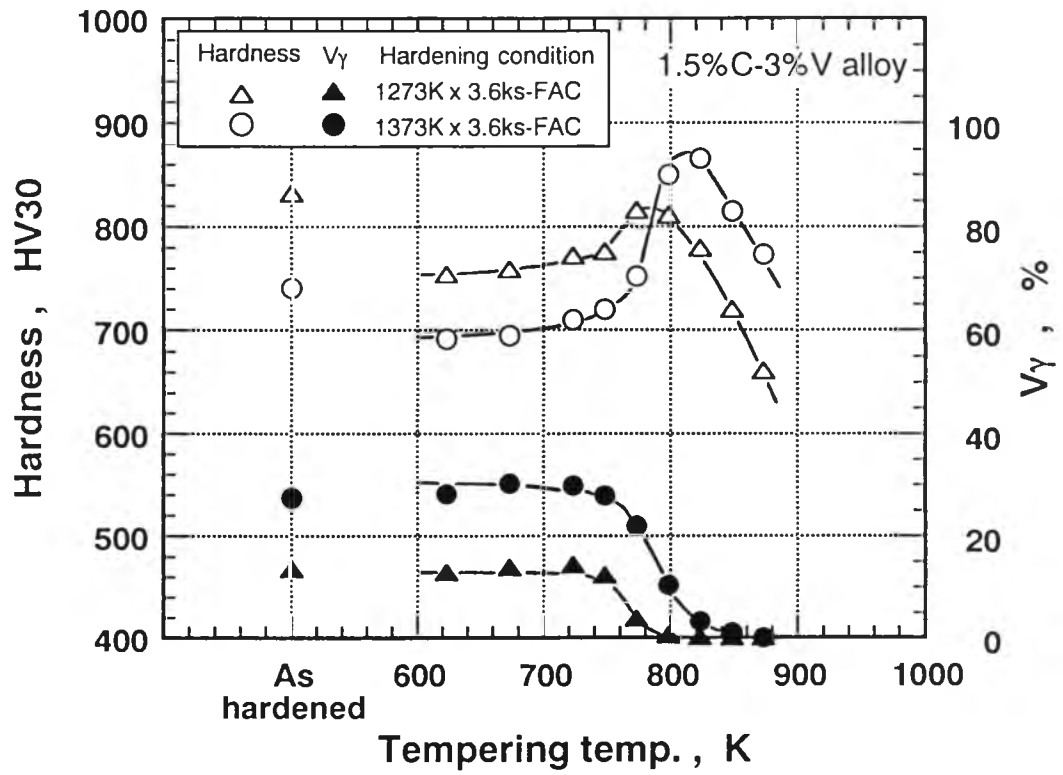


Fig. 4-11 Relationship between macro-hardness and volume fraction of retained austenite( $V_\gamma$ ) and tempering temperature. (Specimen No.8)

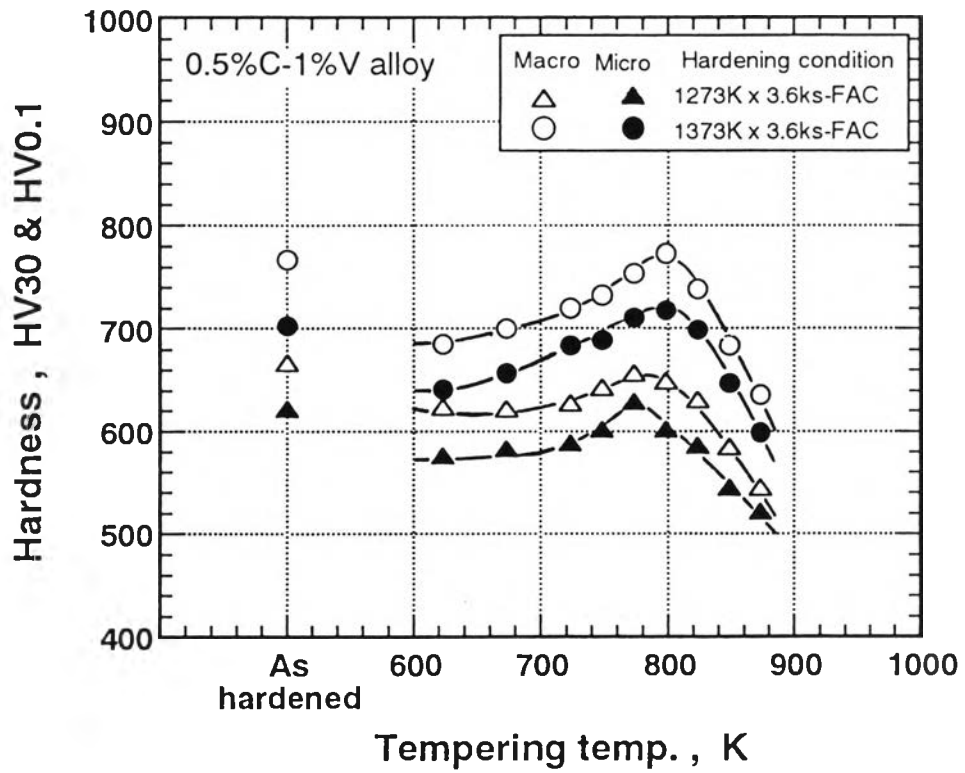


Fig. 4-12 Comparison of micro-hardness in matrix with macro-hardness. (Specimen No.1)

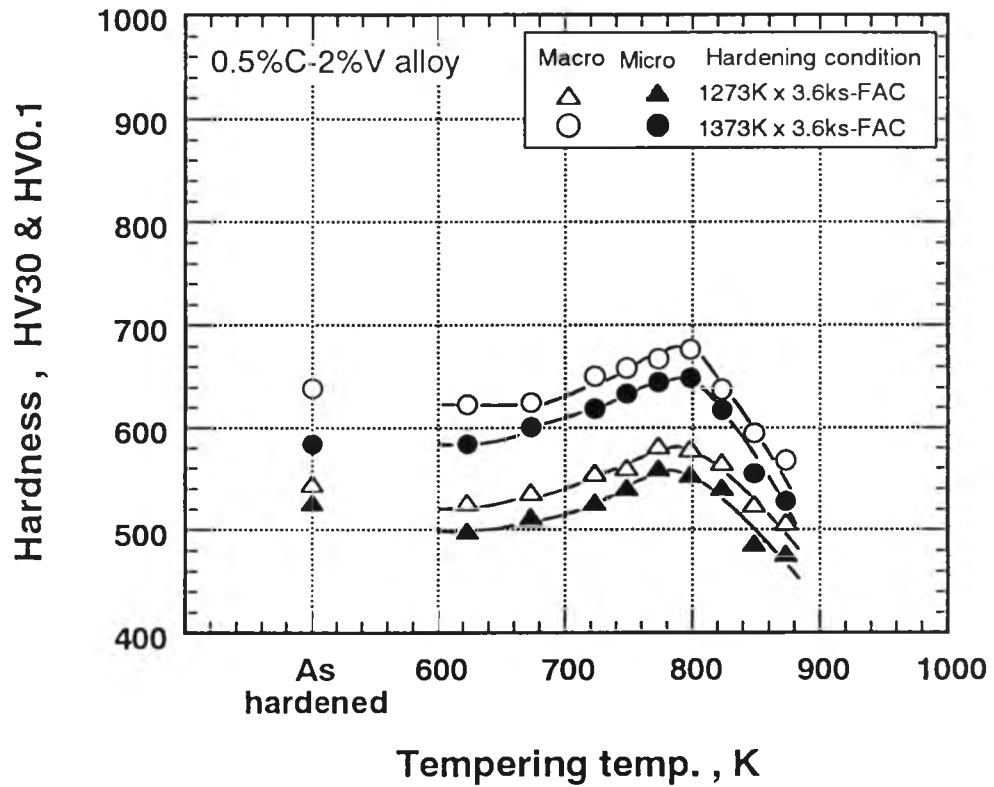


Fig. 4-13 Comparison of micro-hardness in matrix with macro-hardness. (Specimen No.2)

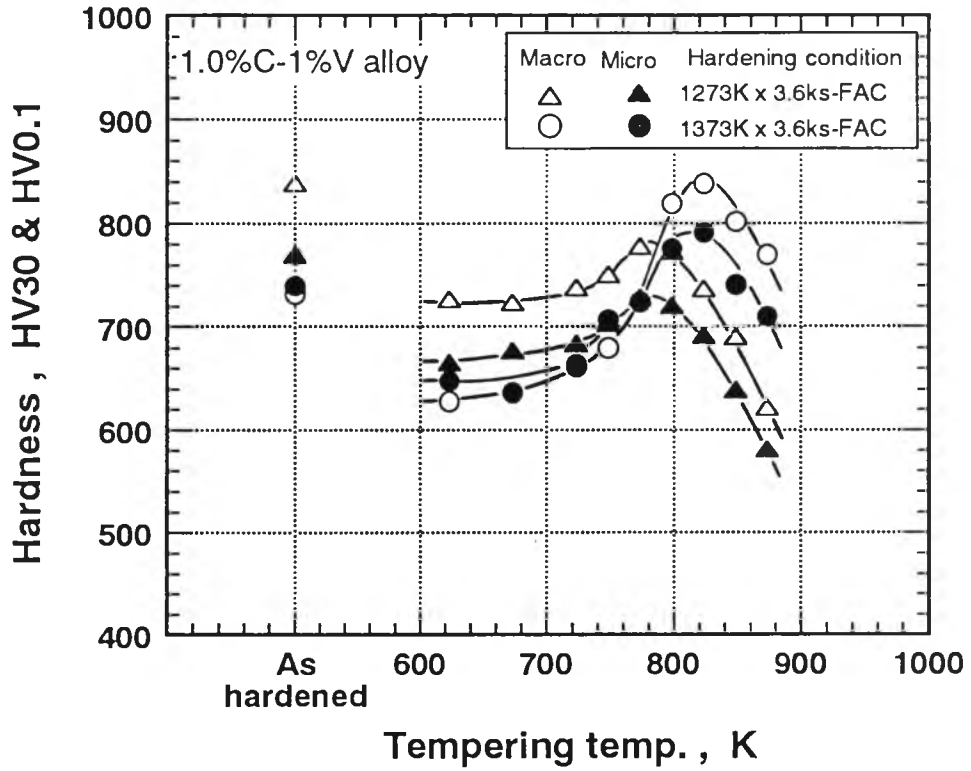


Fig. 4-14 Comparison of micro-hardness in matrix with macro-hardness. (Specimen No.3)

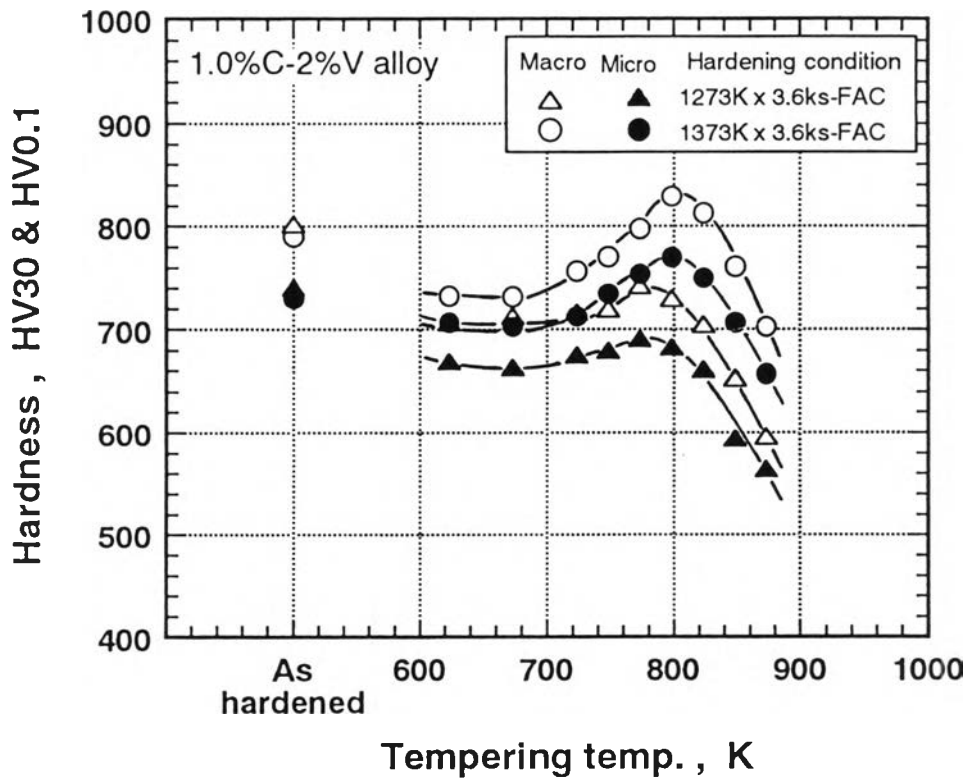


Fig. 4-15 Comparison of micro-hardness in matrix with macro-hardness. (Specimen No.4)

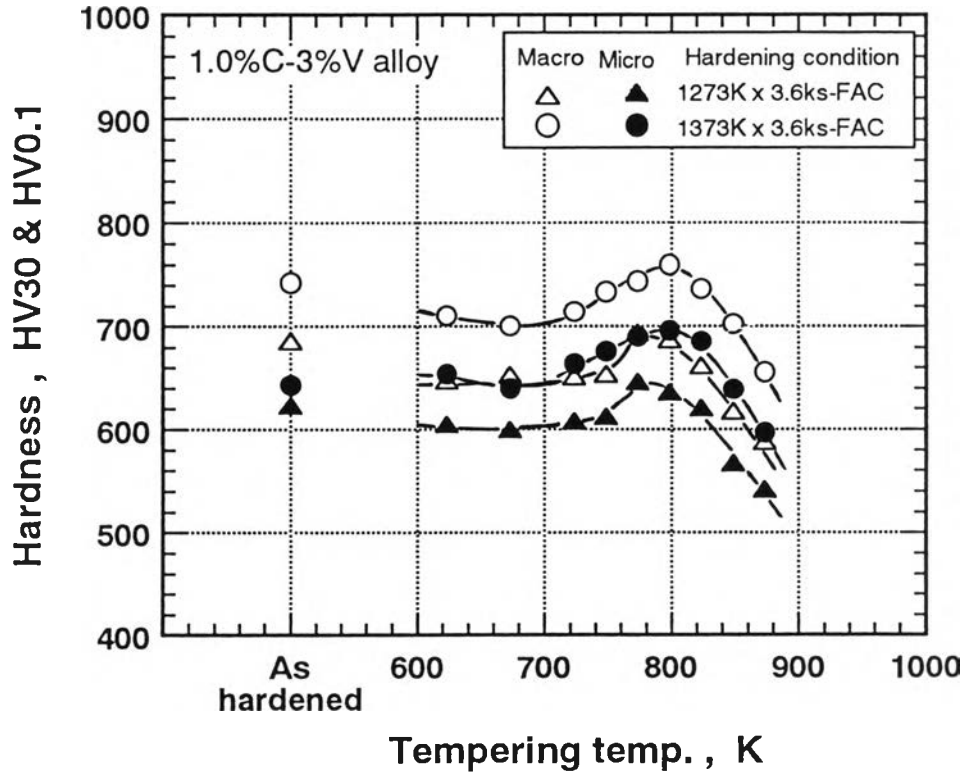


Fig. 4-16 Comparison of micro-hardness in matrix with macro-hardness. (Specimen No.5)



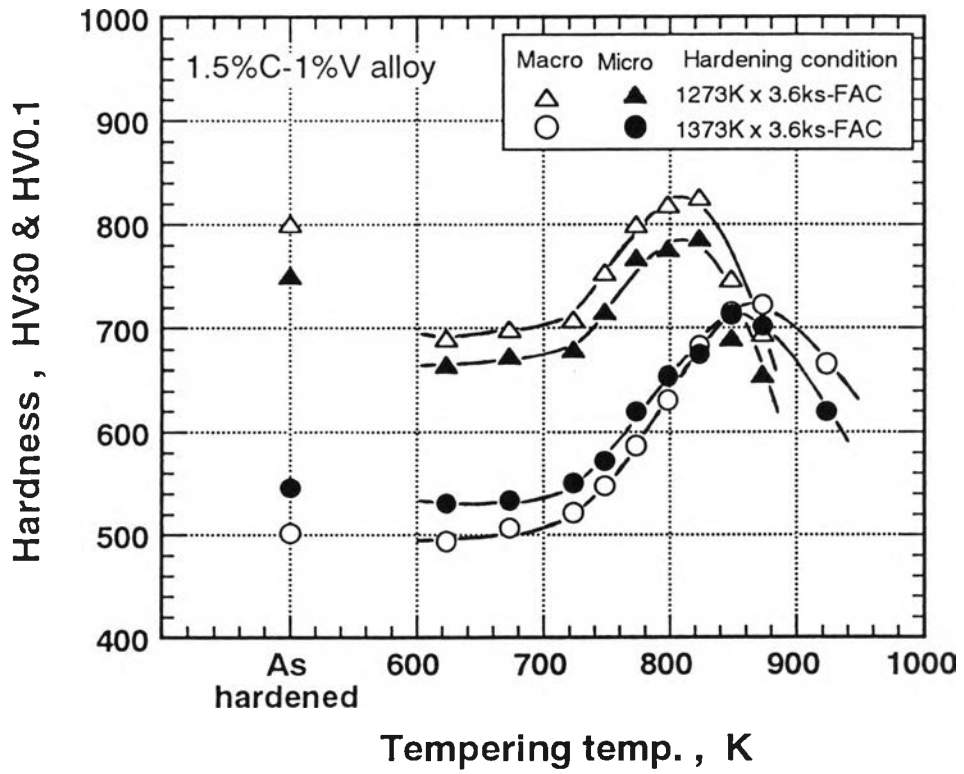


Fig. 4-17 Comparison of micro-hardness in matrix with macro-hardness. (Specimen No.6)

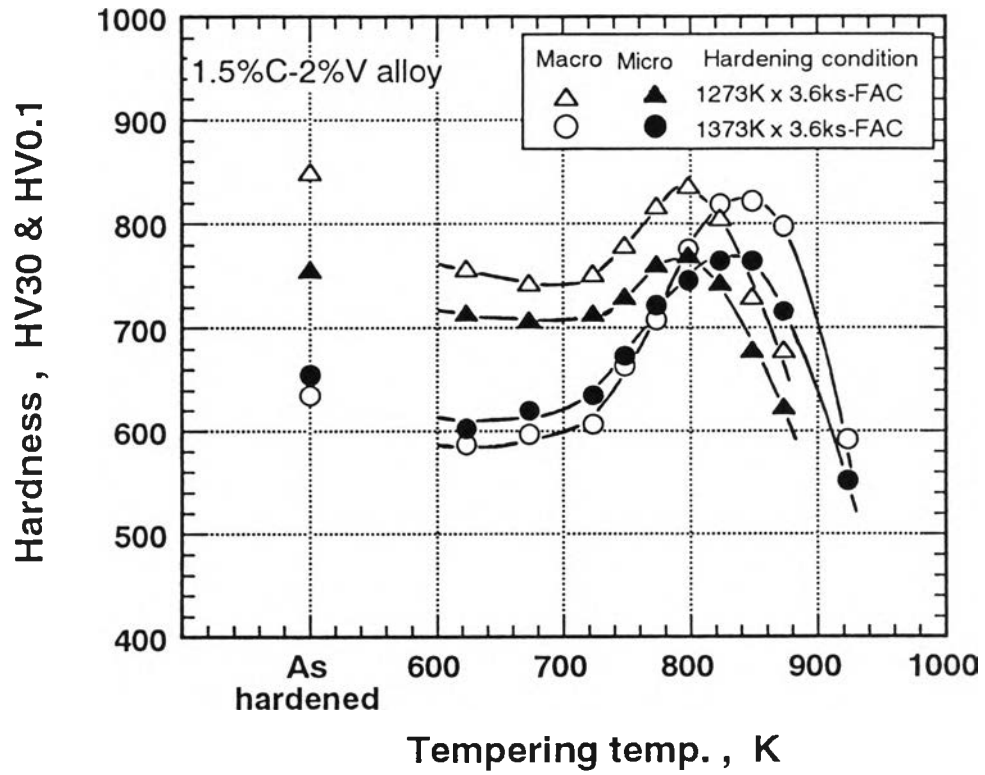


Fig. 4-18 Comparison of micro-hardness in matrix with macro-hardness. (Specimen No.7)

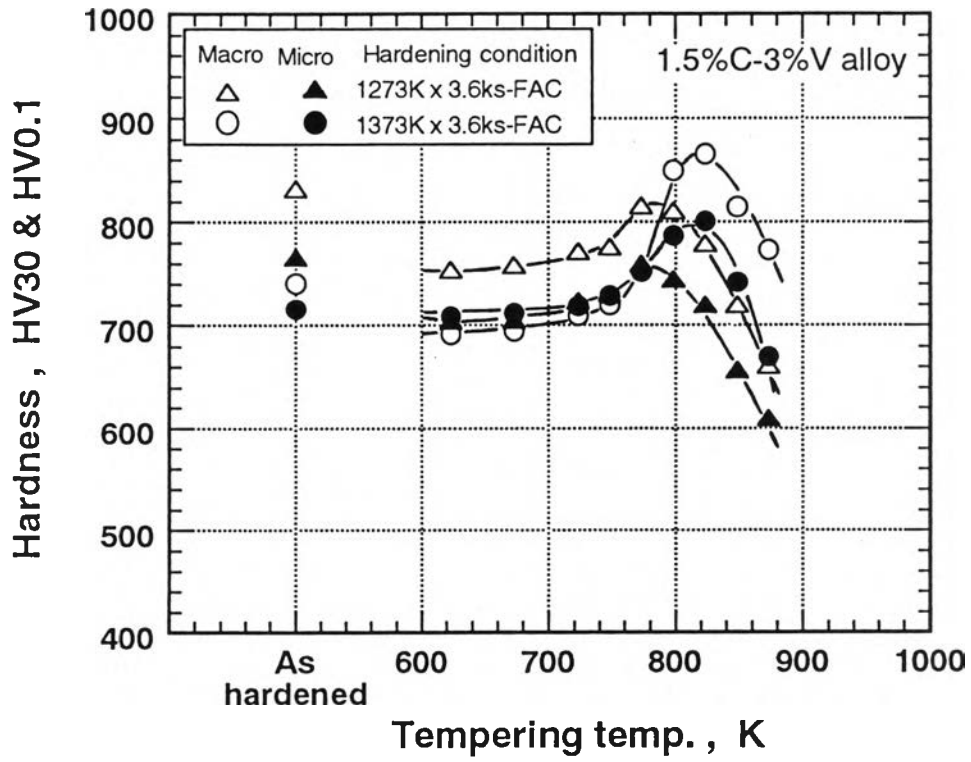


Fig. 4-19 Comparison of micro-hardness in matrix with macro-hardness. (Specimen No.8)